Exploring Primordial Gravitational Waves

Debika Chowdhury

INSPIRE Faculty Fellow, Indian Institute of Astrophysics, Bengaluru

This talk is based on:

D. Chowdhury, G. Tasinato, and I. Zavala, JCAP 08, 010 (2022).
D. Chowdhury, G. Tasinato, and I. Zavala, Phys. Rev. D 107, 083516 (2023).
D. Chowdhury, G. Tasinato, and I. Zavala, JCAP 11, 090 (2023).
A. Marriott-Best, **D. Chowdhury**, A. Ghoshal, and G. Tasinato, Phys. Rev. D 111, 103001 (2025).
B. Atkins, **D. Chowdhury**, A. Marriott-Best, and G. Tasinato, Phys. Rev. D 112, 063534 (2025).

IIT Madras
February 19, 2026

Outline of the talk

- Introduction
- Primordial Gravitational Waves (PGWs)
- PGWs in modified cosmological scenarios
- Induced GWs
- GW detection
- Anisotropies in the Stochastic GW Background (SGWB)
- Summary

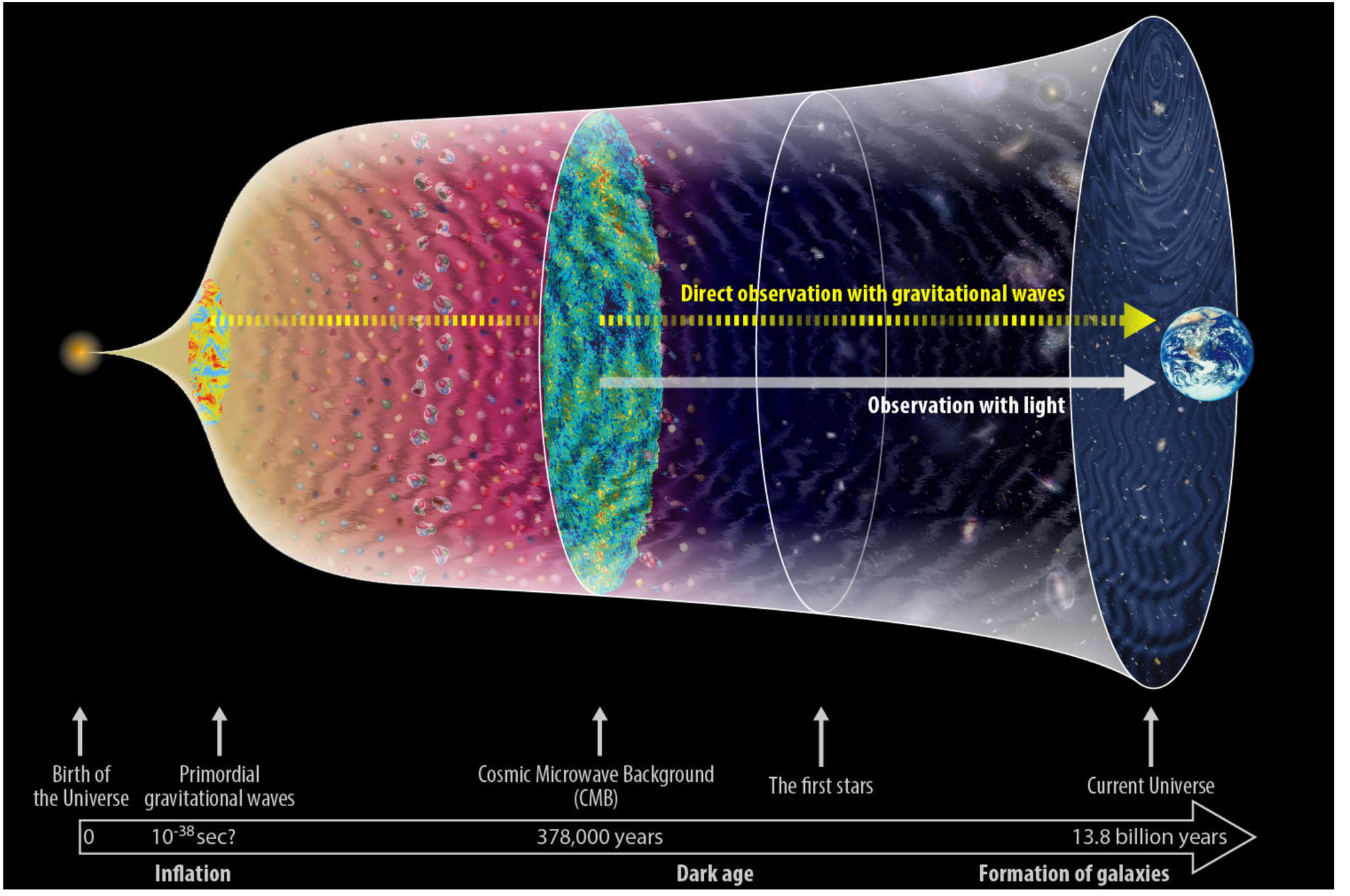

Image from: https://gwpo.nao.ac.jp/en/gallery/oooo61.html.

The Gravitational Wave Spectrum

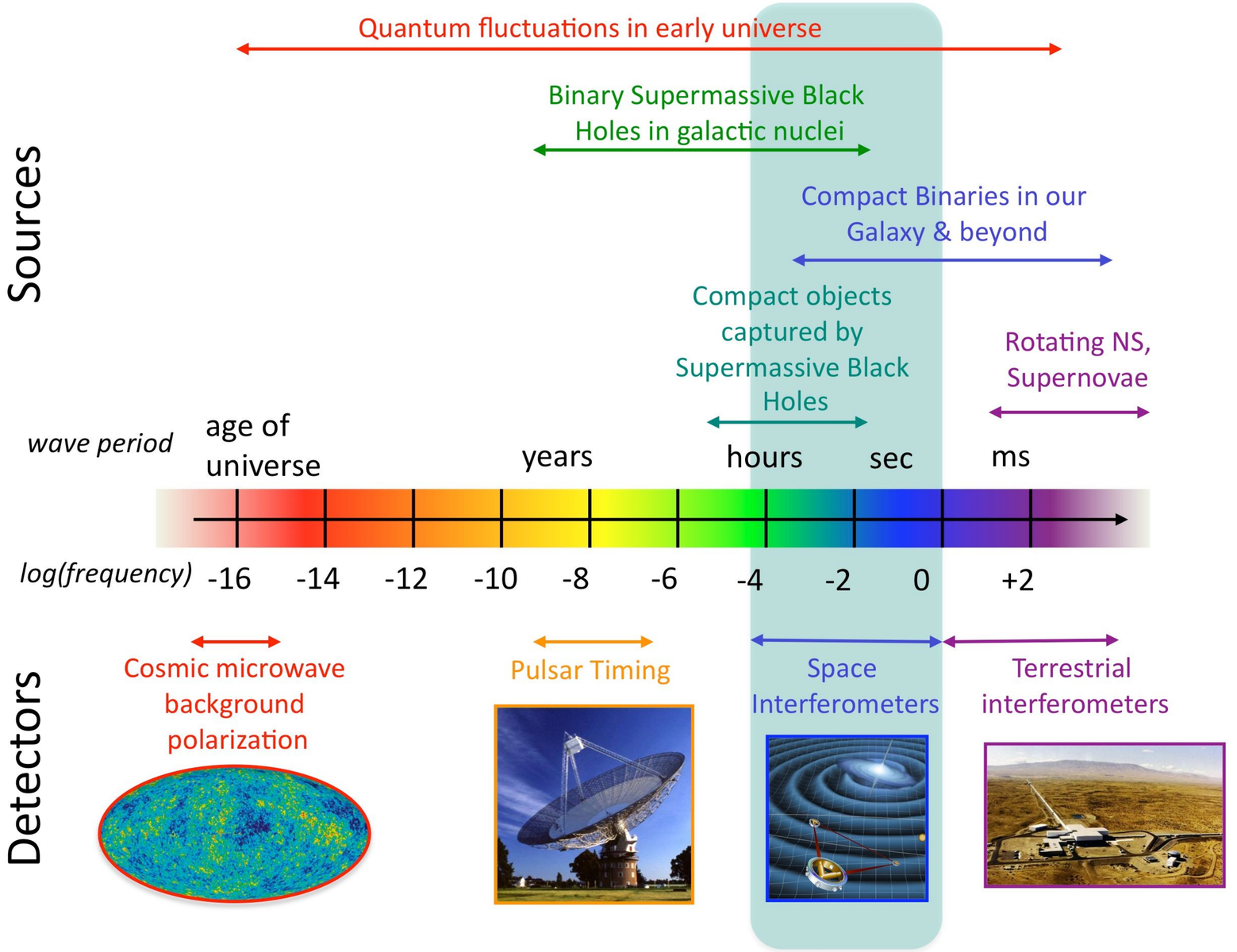

Image from: https://science.gsfc.nasa.gov/663/research/.

Stochastic Gravitational Wave Background

A Stochastic Gravitational Wave Background (SGWB) can be broadly defined as:
"... a random gravitational-wave signal produced by a large number of weak, independent, and unresolved sources."

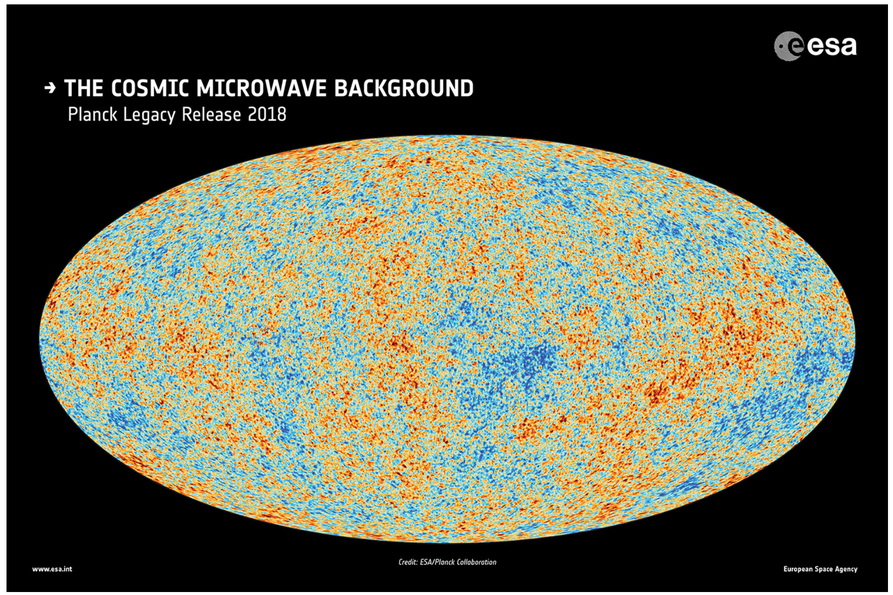

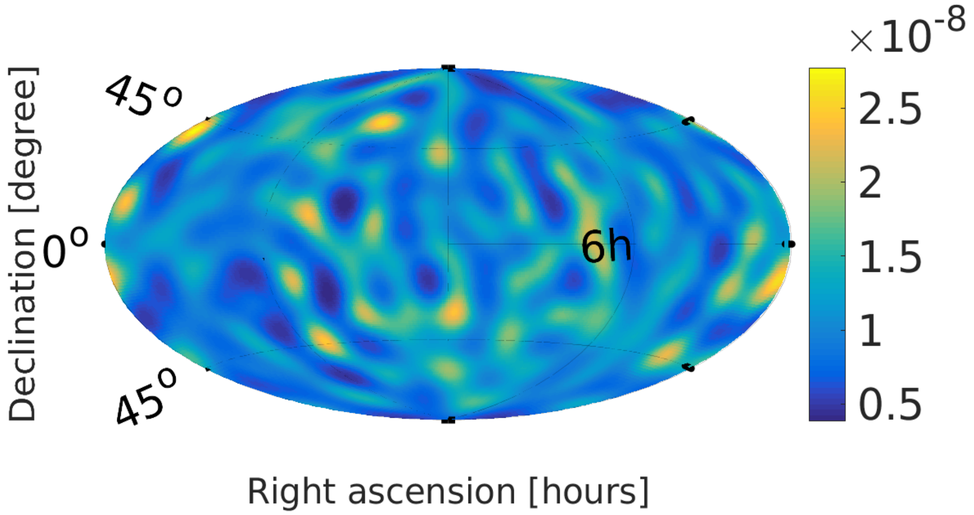

Left: Planck's view of the cosmic microwave background.
Right: Energy density of the gravitational-wave background from Advanced LIGO's First Observing Run.

J. D. Romano and N. J. Cornish, Living Rev. Rel. 20, 2 (2017); B. P. Abbott et al., Phys. Rev. Lett. 118, 121102 (2017).
Planck image from: https://www.esa.int/ESA_Multimedia/Images/2018/07/Planck_s_view_of_the_cosmic_microwave_background2.

Primordial Gravitational Waves

Generation of PGWs

Equation of motion for primordial tensor fluctuations:

$$\ddot{h}_{ij} + 3H\dot{h}_{ij} - \frac{\nabla^2}{a^2}h_{ij} = 0.$$

To solve for the tensor perturbation, one can write it in Fourier space as

$$h_{ij}(t,\vec{x}) = \sum_{\lambda}\int \frac{d^3k}{(2\pi)^3} h^{\lambda}(t,\vec{k})\epsilon^{\lambda}_{ij}(\vec{k})e^{i\vec{k}\cdot\vec{x}}\,.$$

Energy density of the relic GW:

$$\rho_{\rm GW}(t) = \frac{1}{16\pi G}\sum_{\lambda}\int \frac{d^3k}{(2\pi)^3}\,|\,\dot{h}^{\lambda}(t,\vec{k})\,|^2\,.$$

Y. Watanabe and E. Komatsu, Phys. Rev. D 73, 123515 (2006); K. Saikawa and S. Shirai, JCAP 05, 035 (2018); N. Bernal and F. Hajkarim, Phys. Rev. D 100, 063502 (2019); N. Bernal et al., JCAP 11, 015 (2020).

Primordial Gravitational Waves

Generation of PGWs

Relic density of the PGWs:

$$\Omega_{\rm GW}(t,k) = \frac{1}{\rho_c(t)} \frac{d\rho_{\rm GW}(t,k)}{d\ln k} \,.$$

Fractional energy density in primordial gravitational waves, observed today:

$$\Omega^0_{\rm GW}(k)\, h^2 \simeq \frac{1}{24}\, \mathscr{P}_{\rm T}(k) \left(\frac{g_{*s,0}}{g_{*s,\rm hc}}\right)^{4/3} \left(\frac{T_0}{T_{\rm hc}}\right)^4 \left(\frac{H_{\rm hc}}{H_0/h}\right)^2 .$$

Frequency of GWs observed today:

$$f_0 = 2.61745 \times 10^{-8} \left(\frac{g_{*s,\rm hc}}{100}\right)^{-1/3} \left(\frac{g_{*,\rm hc}}{100}\right)^{1/2} \left(\frac{T_{\rm hc}}{1\,\text{GeV}}\right) \text{Hz} \,.$$

Sources of PGWs

There are broadly two types of sources of PGWs.

Primary GWs

- Inflation
- Reheating
- Post-inflationary dynamics

Induced GWs

- Scalar-induced GWs
- GWs induced by primordial magnetic fields

Modified cosmological scenarios

Action

$$S = S_{\rm EH} + S_\phi + S_m,$$

where

$$S_{\rm EH} = \frac{1}{2\kappa^2}\int {\rm d}^4x\sqrt{-g}\,R,$$

$$S_\phi = -\int {\rm d}^4x\sqrt{-g}\left[\frac{b}{2}(\partial\phi)^2 + M^4C^2(\phi)\sqrt{1+\frac{D(\phi)}{C(\phi)}\left(\partial\phi\right)^2} + V(\phi)\right],$$

$$S_m = -\int {\rm d}^4x\sqrt{-\tilde{g}}\,\mathscr{L}_M(\tilde{g}_{\mu\nu})\,.$$

B. Dutta, E. Jimenez, and I. Zavala, JCAP 06, 032 (2017); B. Dutta, E. Jimenez, and I. Zavala, Phys. Rev. D 96, 103506 (2017).

Modified cosmological scenarios

Equations of motion:

$$H^2 = \frac{\kappa^2}{3}\left[\rho_\phi + \rho\right],$$

$$\dot{H} + H^2 = -\frac{\kappa^2}{6}\left[\rho_\phi + 3P_\phi + \rho + 3P\right],$$

$$\ddot{\phi}\left[1 + \frac{b}{M^4 CD\gamma^3}\right] + 3H\dot{\phi}\,\gamma^{-2}\left[\frac{b}{M^4 CD\gamma} + 1\right] + \frac{C}{2D}\left(\gamma^{-2}\left[\frac{5C'}{C} - \frac{D'}{D}\right] + \frac{D'}{D} - \frac{C'}{C} - 4\gamma^{-3}\frac{C'}{C}\right) + \frac{1}{M^4 CD\gamma^3}\left(\mathscr{V}' + Q_0\right) = 0,$$

where

$$\rho_\phi = -\left[\frac{b}{2} + \frac{M^4 CD\gamma^2}{\gamma + 1}\right](\partial\phi)^2 + \mathscr{V}, \qquad P_\phi = -\left[\frac{b}{2} + \frac{M^4 CD\,\gamma}{\gamma + 1}\right](\partial\phi)^2 - \mathscr{V}, \qquad \gamma = (1 - D\,\dot{\phi}^2/C)^{-1/2}.$$

B. Dutta, E. Jimenez, and I. Zavala, JCAP 06, 032 (2017); B. Dutta, E. Jimenez, and I. Zavala, Phys. Rev. D 96, 103506 (2017).

Modified cosmological scenarios

Evolution of the equation of state

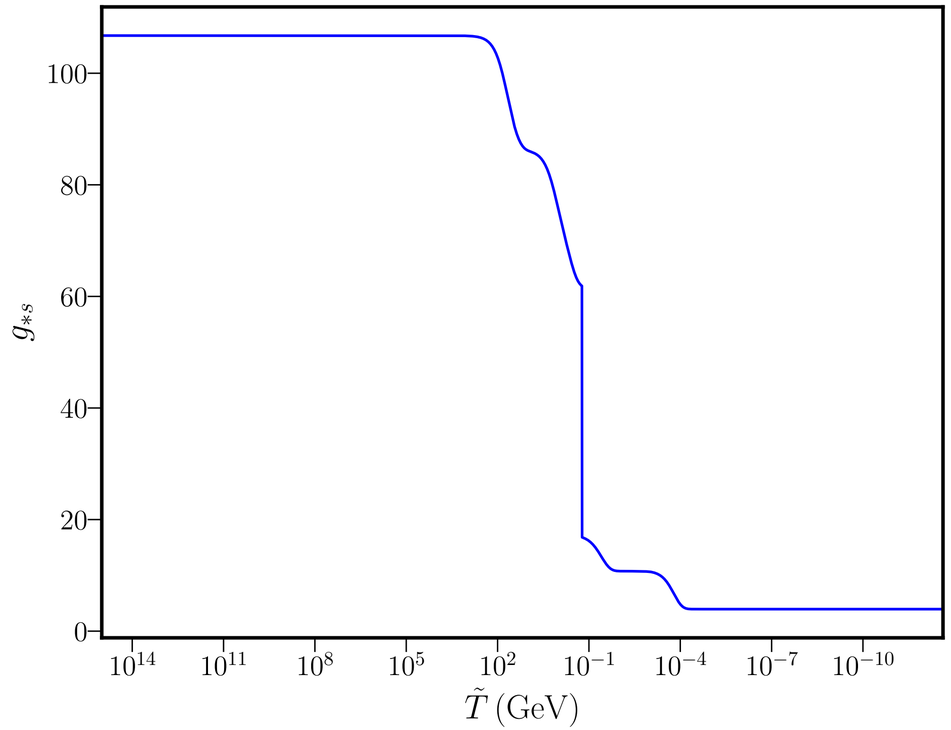

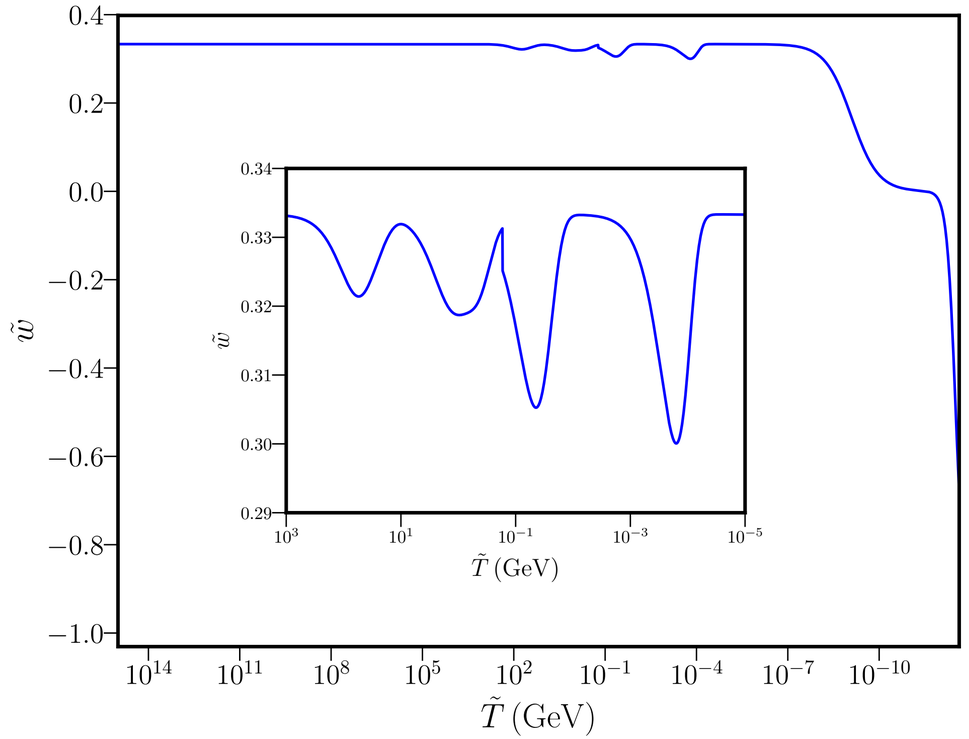

Behaviour of g_{*s} and the equation of state.

D. Chowdhury, G. Tasinato, and I. Zavala, JCAP 08, 010 (2022).

Modified cosmological scenarios

Evolution of the scalar field

Normalization condition: $M^4CD = 1.$

Case 1: $C = 1.$

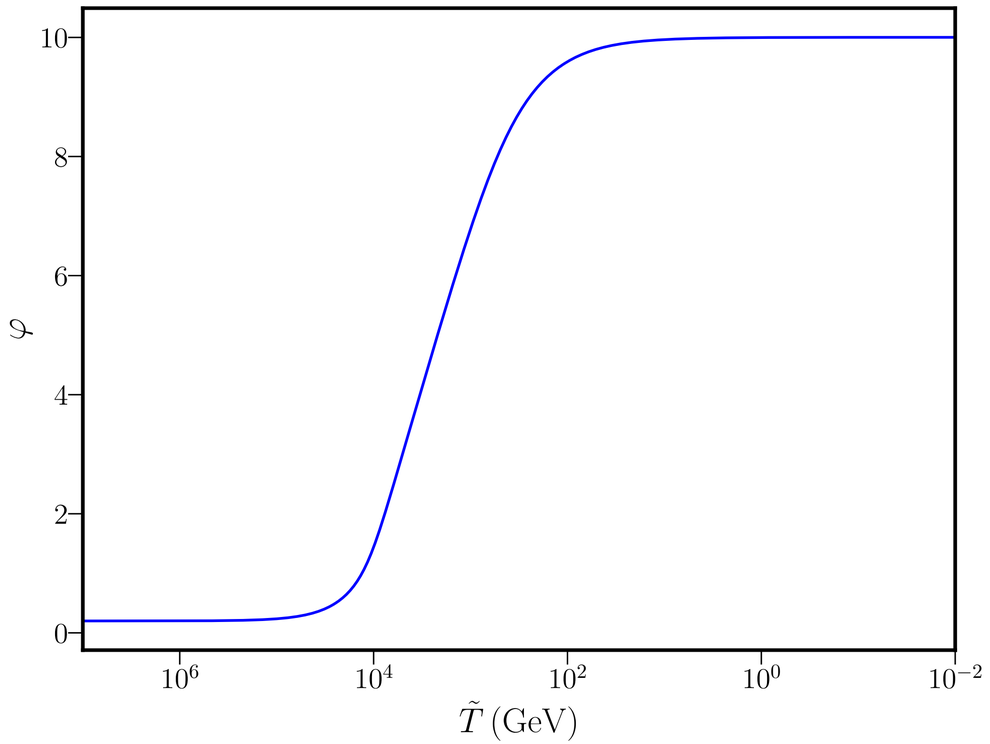

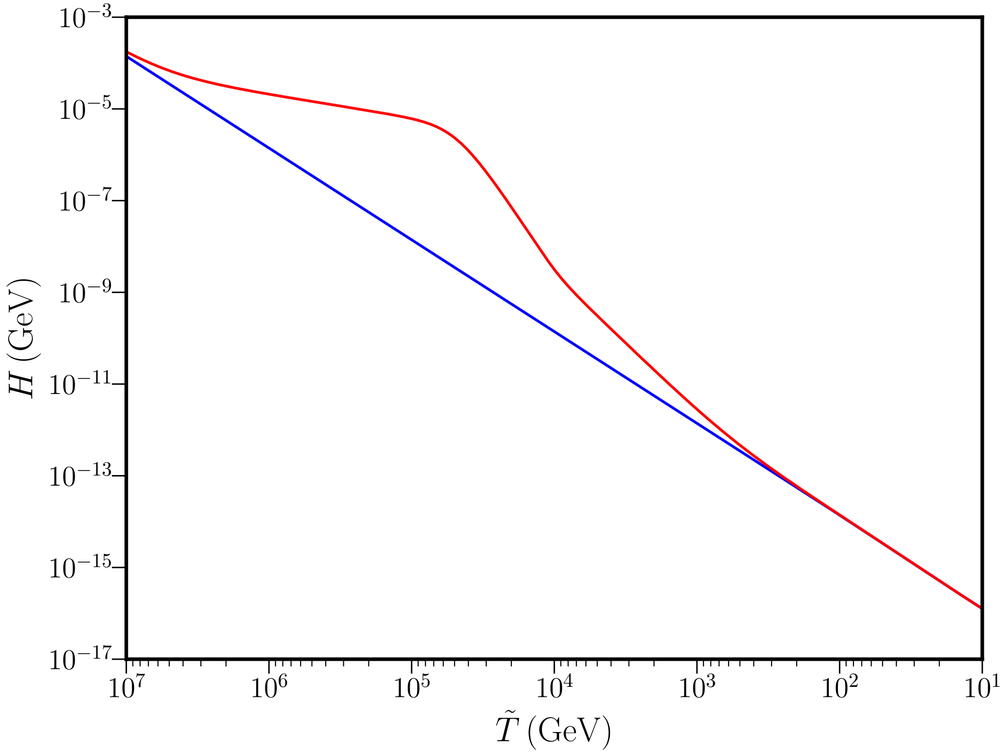

Evolution of the field (left) and the expansion rate (right).

Modified cosmological scenarios

Evolution of the energy density

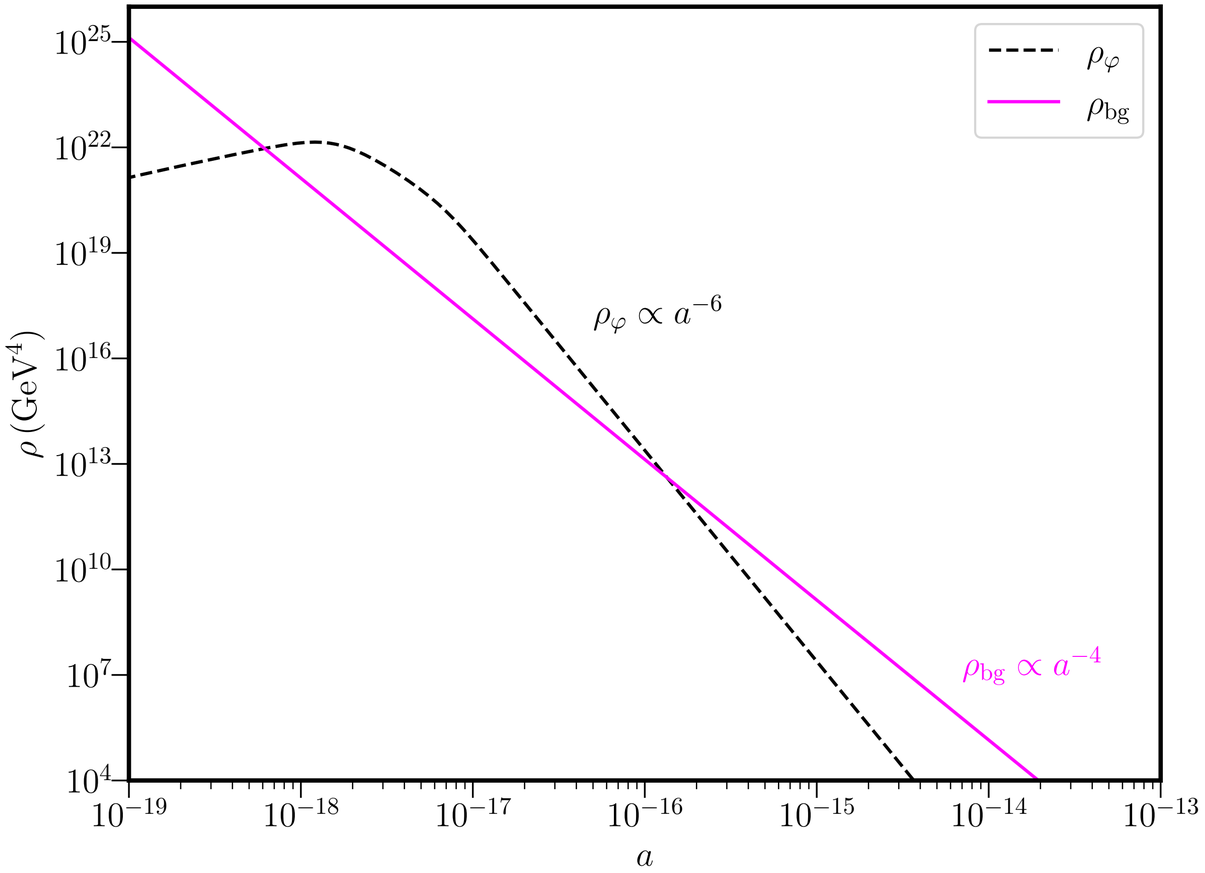

Energy density vs. the scale factor

Modified cosmological scenarios

Primordial GW spectrum

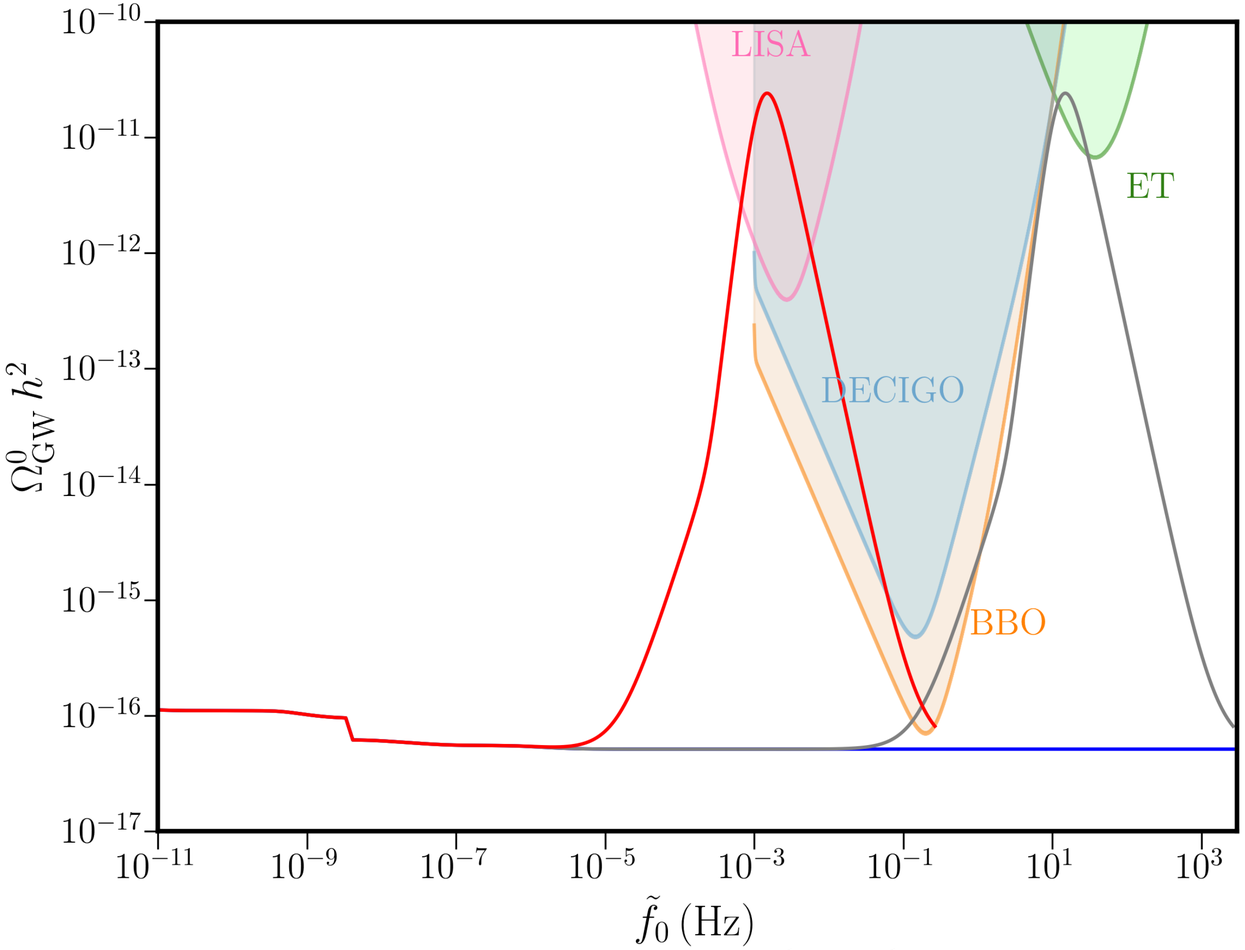

PGW spectrum produced in Case 1.

D. Chowdhury, G. Tasinato, and I. Zavala, JCAP 08, 010 (2022).

Modified cosmological scenarios

Evolution of the scalar field

Case 2: $C(\varphi) = (1 + be^{-\beta\varphi})^{2n}$. We choose $b = 0.1,\ \beta = 8.$

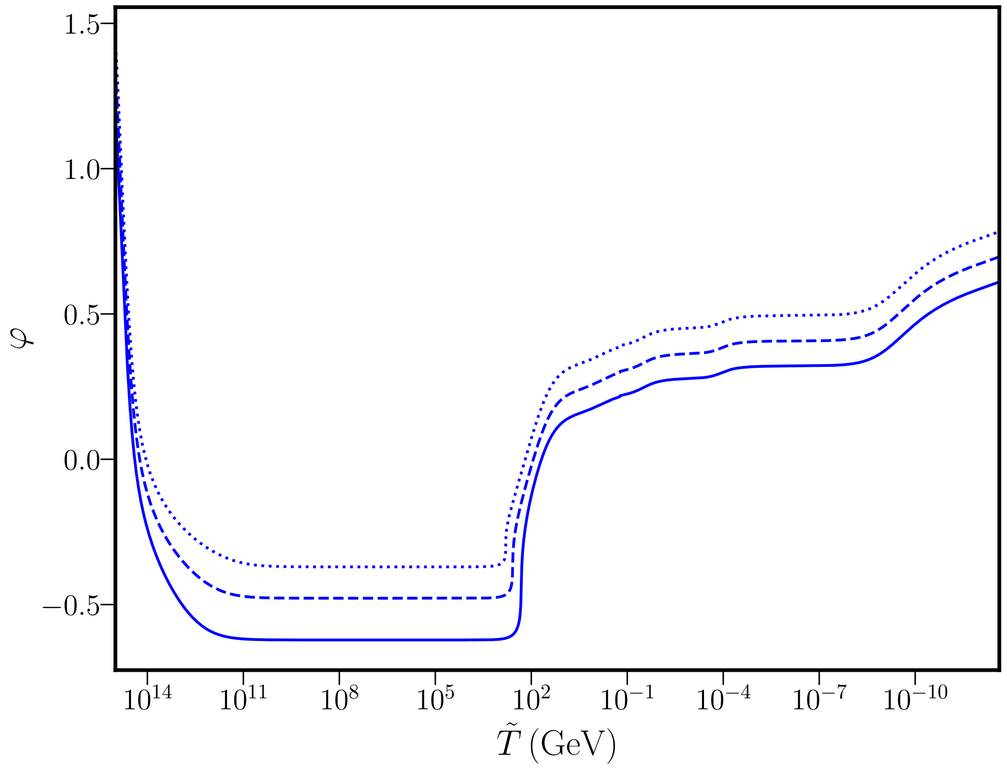

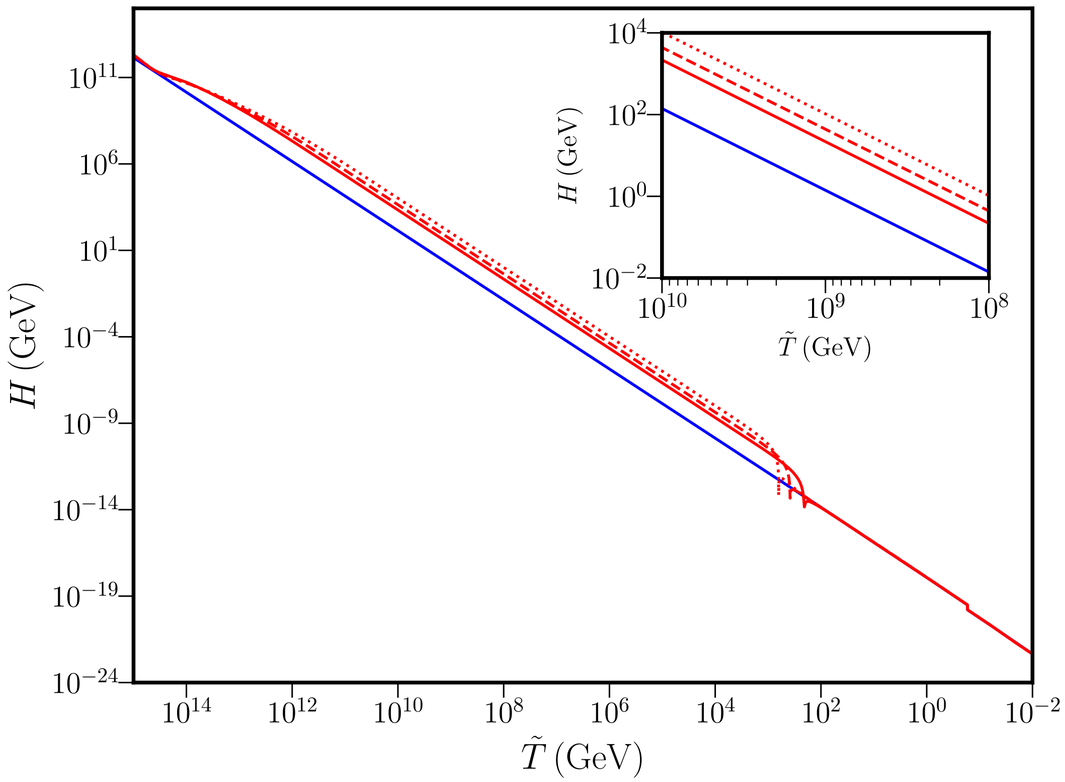

Evolution of the field (left) and the expansion rate (right).

Modified cosmological scenarios

Primordial GW spectrum

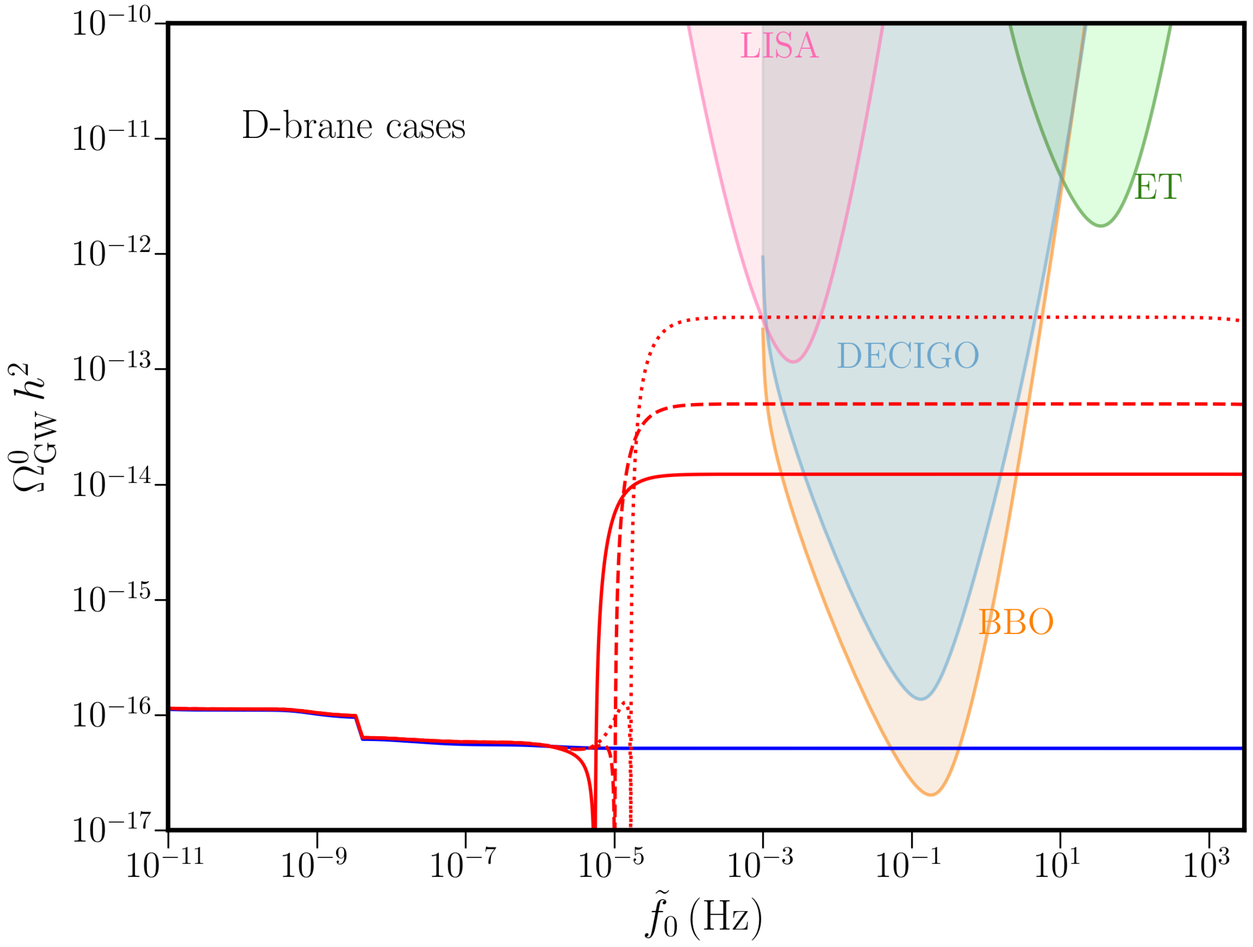

PGW spectrum produced in Case 2.

D. Chowdhury, G. Tasinato, and I. Zavala, JCAP 08, 010 (2022).

Modified cosmological scenarios

Comparison with NANOGrav results

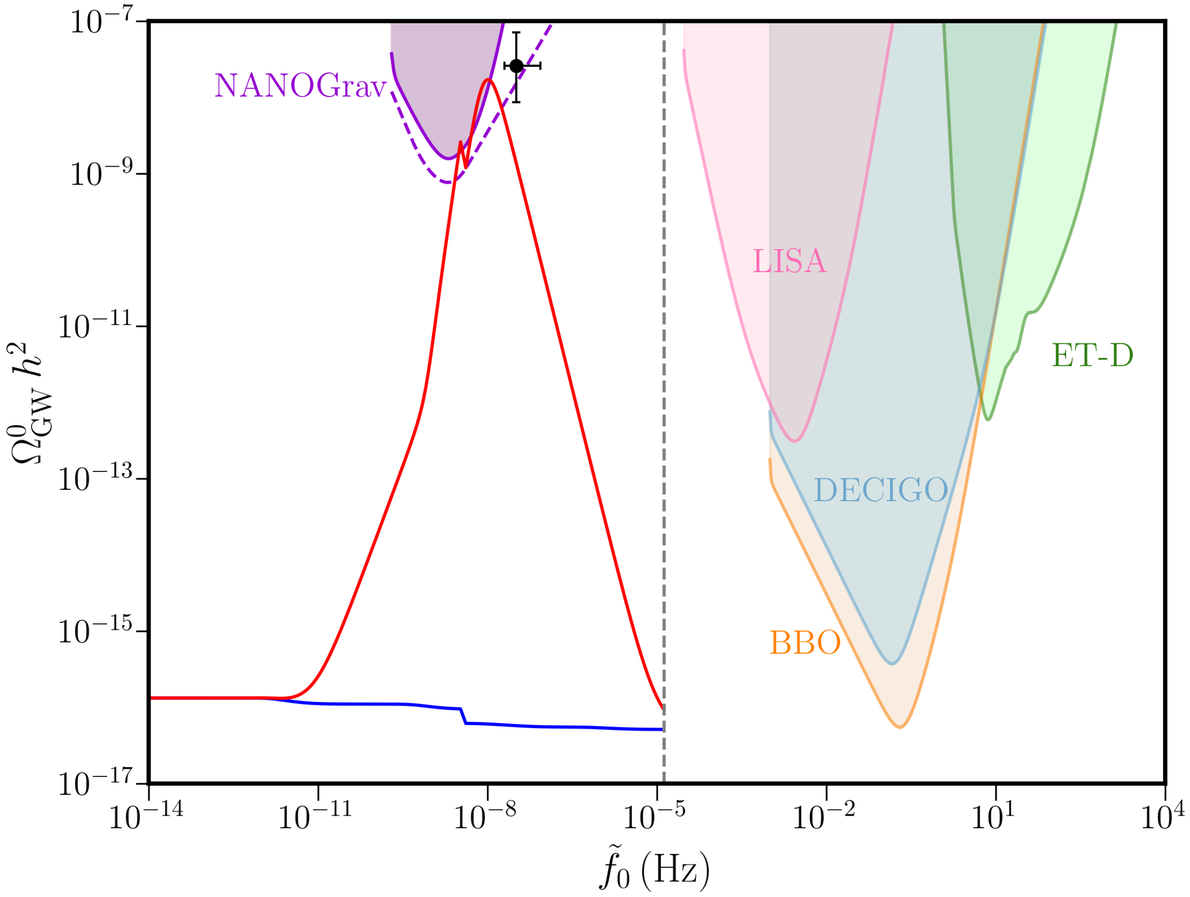

The peak of the PGW spectrum reaches a maximum value of $\sim 1.7 \times 10^{-8}$, in agreement with the NANOGrav bound.

D. Chowdhury, G. Tasinato, and I. Zavala, JCAP 11, 090 (2023).

Modified cosmological scenarios

Parameter estimation

We fit the peak of our spectrum with

$$\tilde{\Omega}^0_{\rm GW}\, h^2 = A_{\rm b}^2\, f^2 \left(\frac{f}{f_{\rm yr}}\right)^{\sigma-3} \left[1+\left(\frac{f}{f_{\rm b}}\right)^{1/\varepsilon}\right]^{\varepsilon(\mu-\sigma)},$$

where $f_{\rm yr} = 1/\text{year}$ in Hz.

We find: $\log_{10}(A_{\rm b}/{\rm s}) = 5.279,\ \log_{10}(f_{\rm b}/{\rm Hz}) = -8.048,\ \sigma = 6.0,\ \varepsilon = 0.25,$ and $\mu = -2.0.$

We vary $\log_{10}(A_{\rm b}/{\rm s})$ and $\log_{10}(f_{\rm b}/{\rm Hz})$ using PTArcade, and find the following best-fit values:

$$\log_{10}(A_{\rm b}/{\rm s}) = 5.242 \pm 0.191,$$
$$\log_{10}(f_{\rm b}/{\rm Hz}) = -8.149 \pm 0.144.$$

D. Chowdhury, G. Tasinato, and I. Zavala, JCAP 11, 090 (2023); *A. Mitridate and D. Wright, PTArcade (https://doi.org/10.5281/zenodo.8106173) (2023); A. Mitridate et al., arXiv: 2306.16377 [hep-ph]; W. G. Lamb, S. R. Taylor, and R. van Haasteren, Phys. Rev. D 108 (10), 103019 (2023).*

Sourcing secondary GWs

The evolution equation for the GW modes is

$$h_{\mathbf{k}}^{(\lambda)\prime\prime} + 2\mathscr{H}\, h_{\mathbf{k}}^{(\lambda)\prime} + k^2\, h_{\mathbf{k}}^{(\lambda)} \;=\; S^{(\lambda)}(\eta, \mathbf{k})\,.$$

The source is

$$S^{(\lambda)}(\eta, \mathbf{k}) = \mathbf{e}^{(\lambda)\,ij}(\hat{k})\,\Pi_{ij}^{(T)}(\eta, \mathbf{k}) \;=\; \frac{2\,\mathbf{e}^{(\lambda)\,ij}(\hat{k})\,\Lambda_{ij}{}^{mn}\tau_{mn}^{(B)}(\mathbf{k})}{a^2(\eta)}\,,$$

where

$$\tau_{ij}^{(B)}(\mathbf{k}) \;=\; \frac{1}{4\pi}\int \frac{d^3p}{(2\pi)^3}\left[B_i(\mathbf{p})B_j(\mathbf{k}-\mathbf{p}) - \frac{\delta_{ij}}{2}B_m(\mathbf{p})B_m(\mathbf{k}-\mathbf{p})\right].$$

Tensor power spectrum

$$\mathscr{P}_h(\eta, k) \equiv \frac{1}{2}\,\frac{k^3}{2\pi^2}\,\sum_{\lambda}\langle h_{\mathbf{k}}^{(\lambda)}(\eta) h_{\mathbf{q}}^{(\lambda)\,*}(\eta)\rangle'_{\mathbf{k}=\mathbf{q}}\,.$$

GW density parameter

$$\Omega_{\rm GW} \equiv \frac{k^2}{12\,a^2H^2}\mathscr{P}_h\,.$$

B. Atkins et al., Phys. Rev. D 112, 063534 (2025).

Induced GWs

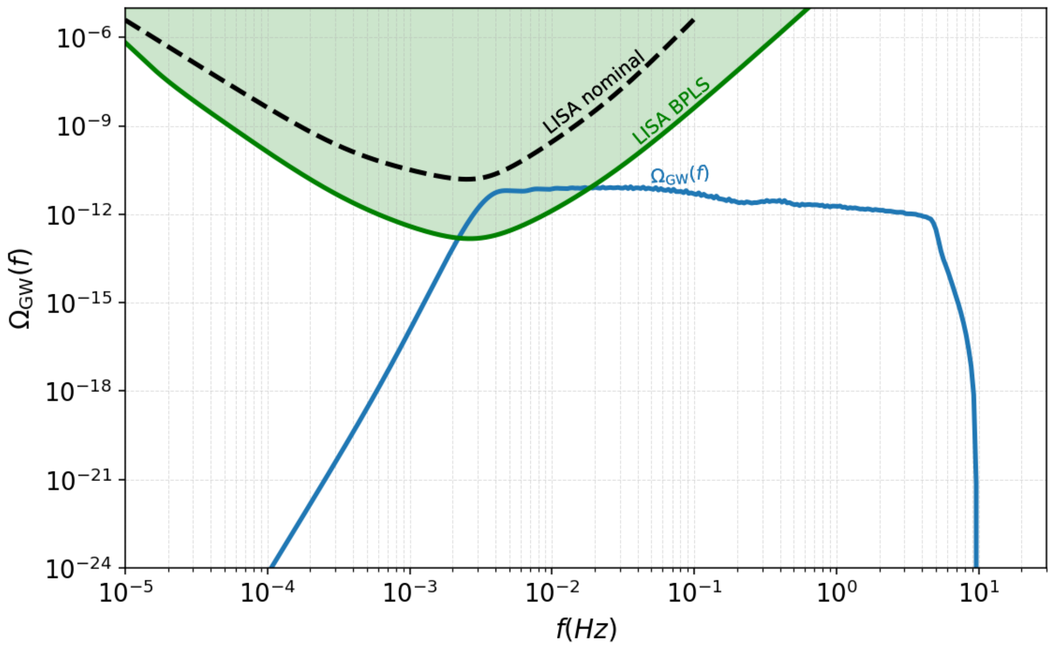

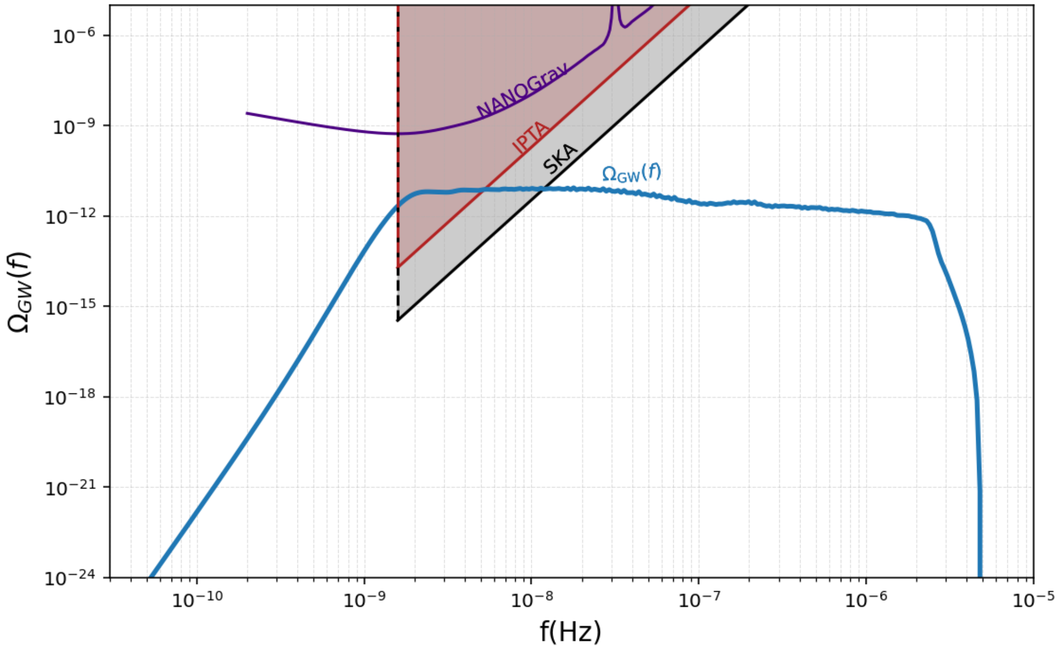

Primordial GWs generated in non-slow-roll magnetogenesis

Plots from: ***B. Atkins et al., Phys. Rev. D 112, 063534 (2025).***

GW detectors

LISA (Laser Interferometer Space Antenna), ET (Einstein Telescope), and CE (Cosmic Explorer) are some of the upcoming third-generation detectors.

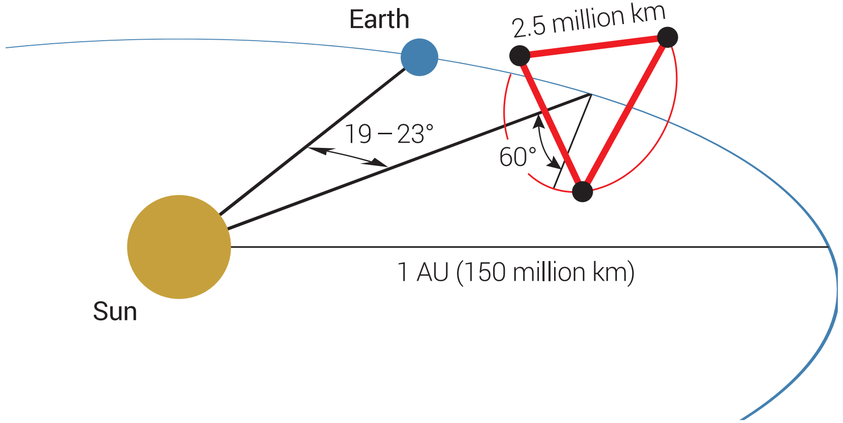

LISA

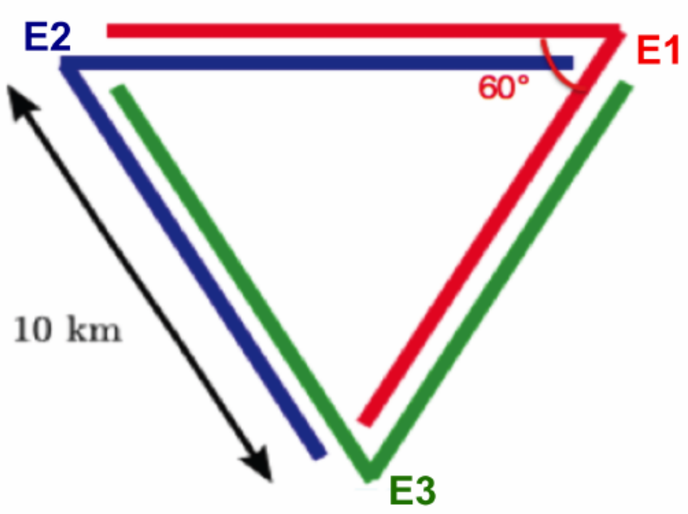

ET

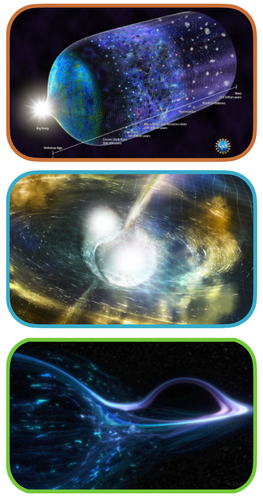

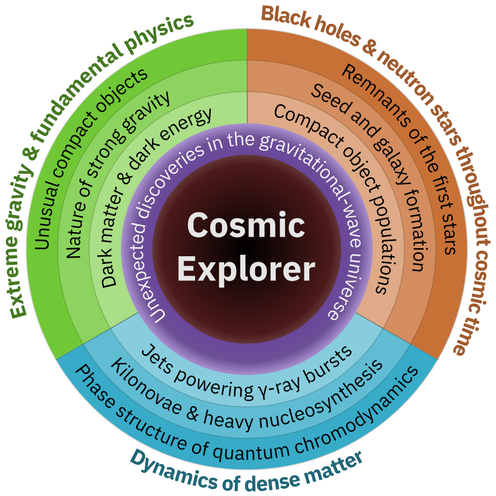

Image from: J. Baker et al., arXiv: 1907.06482 [astro-ph.IM] (2019).

Image from: T. Regimbau et al., Phys. Rev. D 86, 122001 (2012).

Plot from: M. Evans et al., arXiv: 2109.09882 [astro-ph.IM] (2021).

GW detector sensitivities

Sensitivity curves present a convenient visual way of understanding how well a signal can be detected by a particular detector.

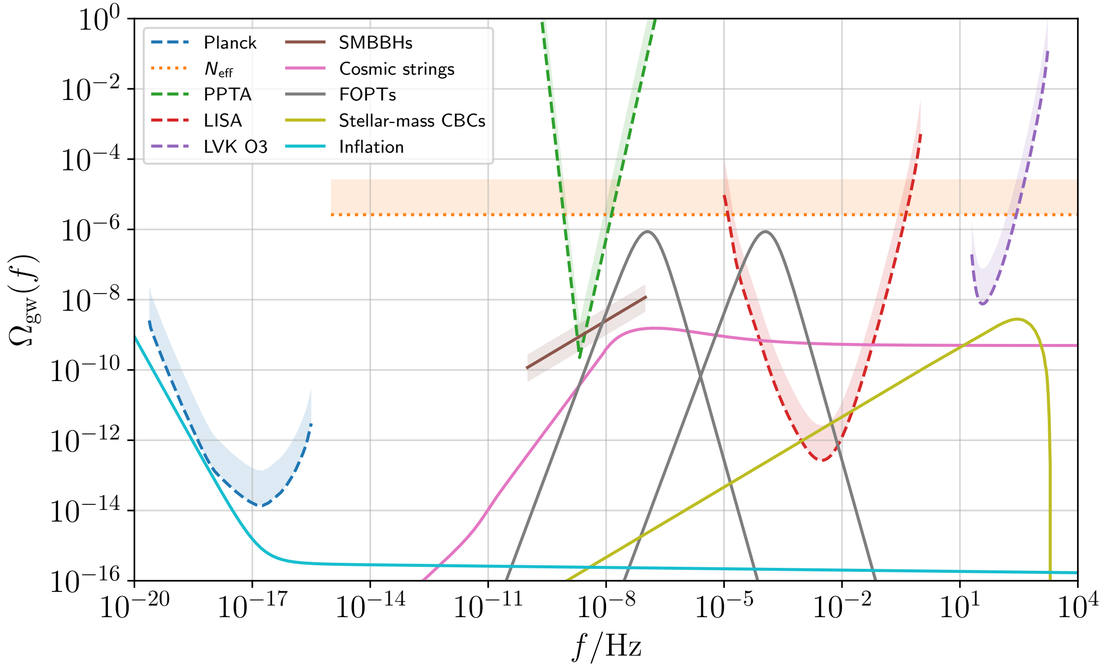

Plot from: A. I. Renzini et al., Galaxies 10, 34 (2022).

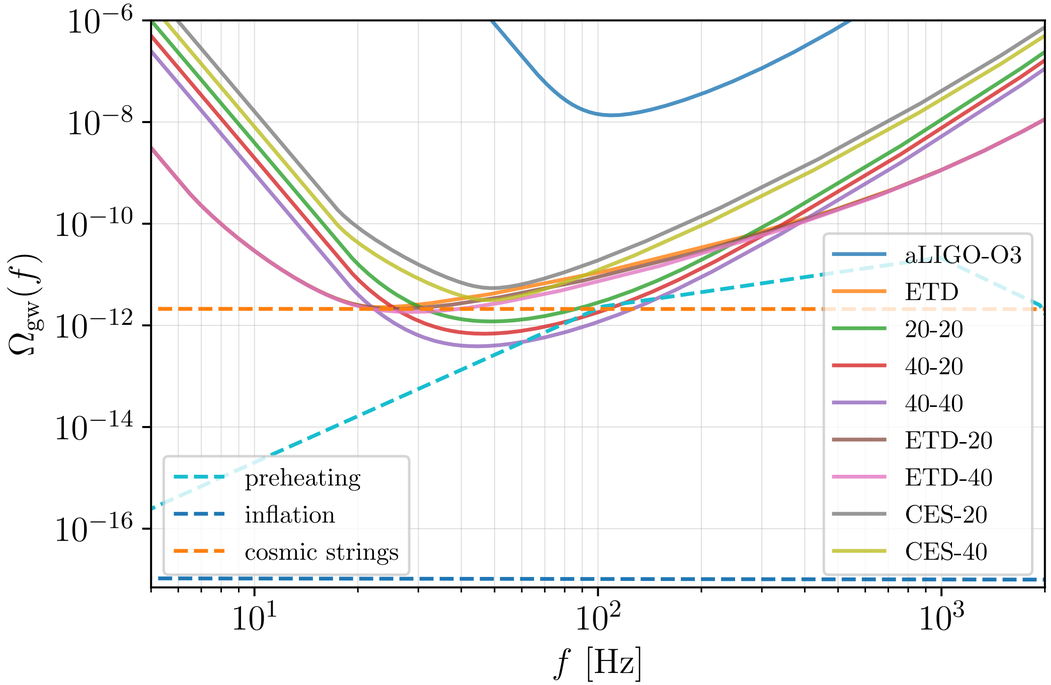

Plot from: M. Evans et al., arXiv: 2109.09882 [astro-ph.IM] (2021).

Power-law integrated sensitivity curves

GW spectra described by the following power-law form are assumed:

$$\Omega_{\mathrm{GW}}(f) = \Omega_\beta \left(\frac{f}{f_*}\right)^\beta .$$

The following amplitude is evaluated:

$$\Omega_\beta = \frac{\rho}{\sqrt{2T}} \left[\int_{f_{\min}}^{f_{\max}} \mathrm{d}f \, \frac{(f/f_*)^{2\beta}}{\Omega_{\mathrm{eff}}^2(f)}\right]^{-1/2} .$$

For each pair (β, Ω_β), $\Omega_{\mathrm{GW}}(f)$ is plotted against f.

The resulting envelope of the family of such curves is the PLS curve

$$\Omega_{\mathrm{GW}}^{\mathrm{PLS}}(f) = \max_\beta \left[\Omega_\beta \left(\frac{f}{f_*}\right)^\beta\right] .$$

E. Thrane and J. D. Romano, Phys. Rev. D 88, 124032 (2013).

Plotting the envelope

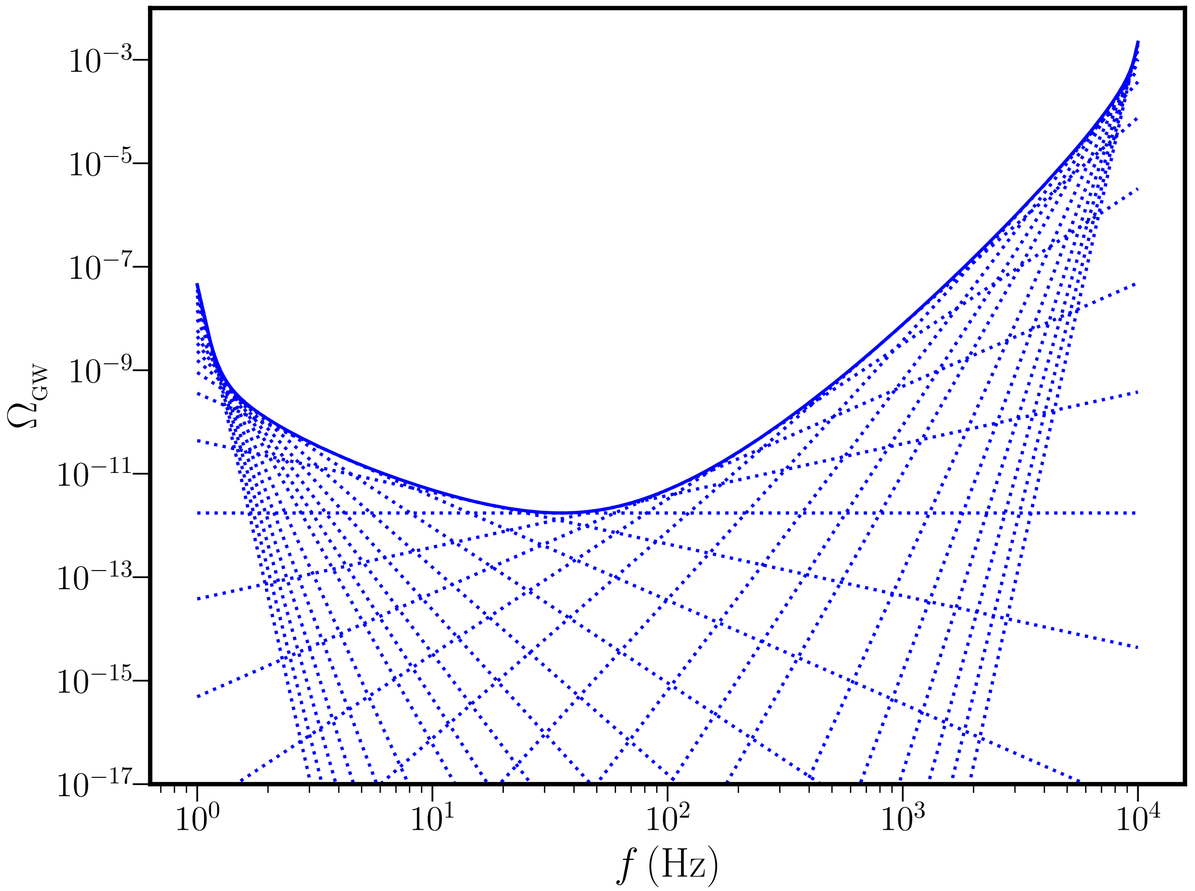

Construction of the PLS for Einstein Telescope

Power-law integrated sensitivity curves

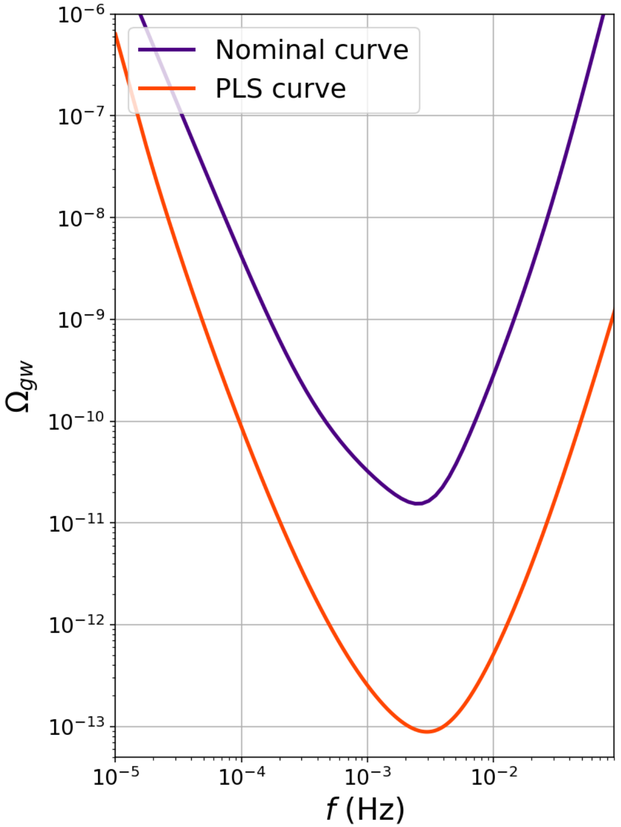

LISA

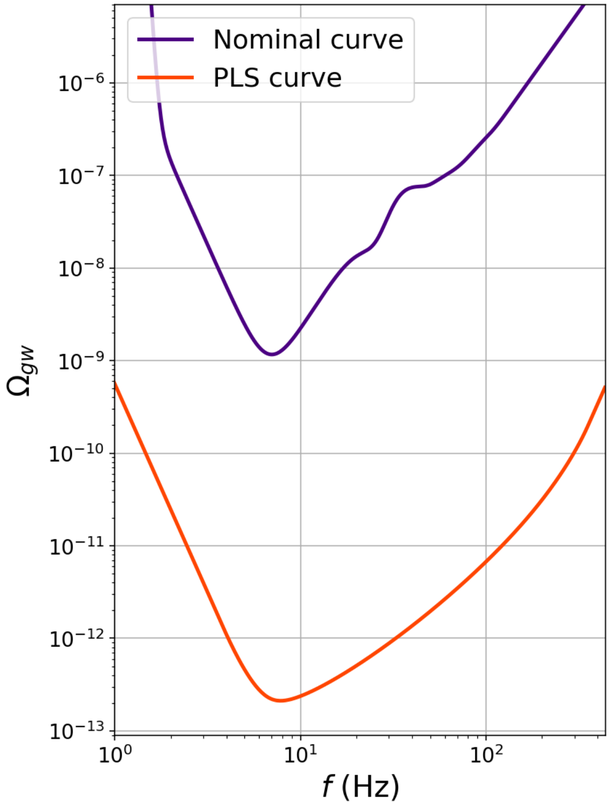

ET

A. Marriott-Best et al., Phys. Rev. D 111, 103001 (2025).

Can we improve the SNR?

The sensitivity of a detector to a particular signal is quantitatively expressed by the signal-to-noise ratio (SNR).

We can combine SNR from different detectors (such as LISA and ET) to improve the sensitivity to broadband signals.

The square of the total SNR is the sum of the squares of the individual SNRs:

$$\mathrm{SNR}_{\mathrm{tot}} = \sqrt{T \int_0^\infty df \left[\frac{\Omega_{\mathrm{GW}}^2(f)}{\Sigma_{\mathrm{LISA}}^2(f)} + \frac{\Omega_{\mathrm{GW}}^2(f)}{\Sigma_{\mathrm{ET}}^2(f)} \right]} = \sqrt{\mathrm{SNR}_{\mathrm{LISA}}^2 + \mathrm{SNR}_{\mathrm{ET}}^2} \,.$$

The two detectors together can reach higher values of SNR.

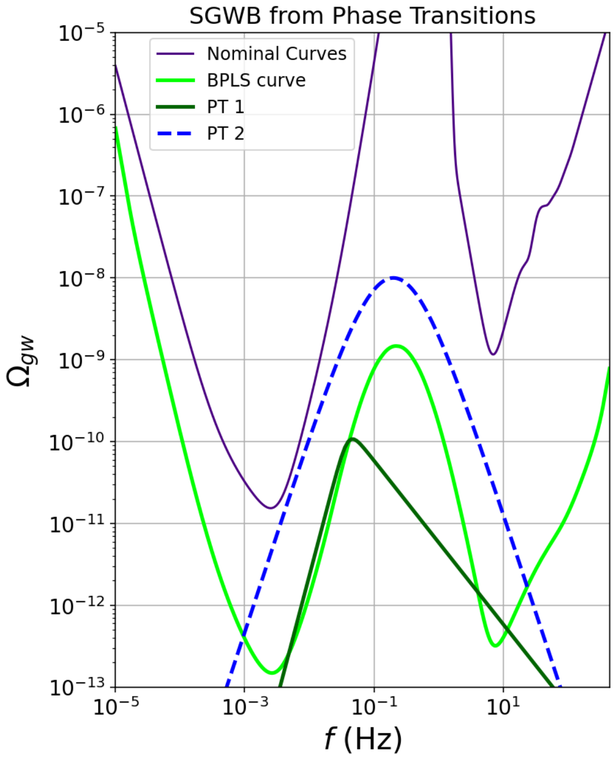

A. Marriott-Best et al., Phys. Rev. D 111, 103001 (2025); *T. L. Smith and R. R. Caldwell, Phys. Rev. D 100, 104055 (2019); J. D. Romano and N. J. Cornish, Living Rev. Rel. 20, 2 (2017).*

GW anisotropies

$\Omega_{\rm GW}$ is characterized by an isotropic and a direction-dependent component.

Anisotropies can be generated at production of GWs or during their propagation.

Example: $$\mathcal{P}_{\mathcal{R}}(k)\,|_{k\gg k_{\rm CMB}} = \frac{A_{\mathcal{R}}}{\sqrt{2\pi}\Delta}\exp\left[-\frac{\ln^2(k/k_*)}{2\Delta^2}\right].$$

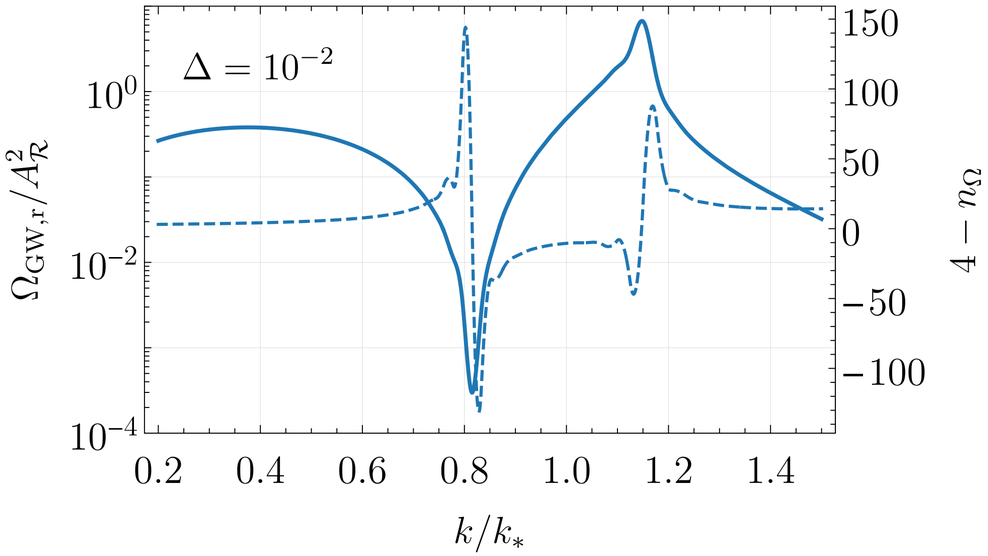

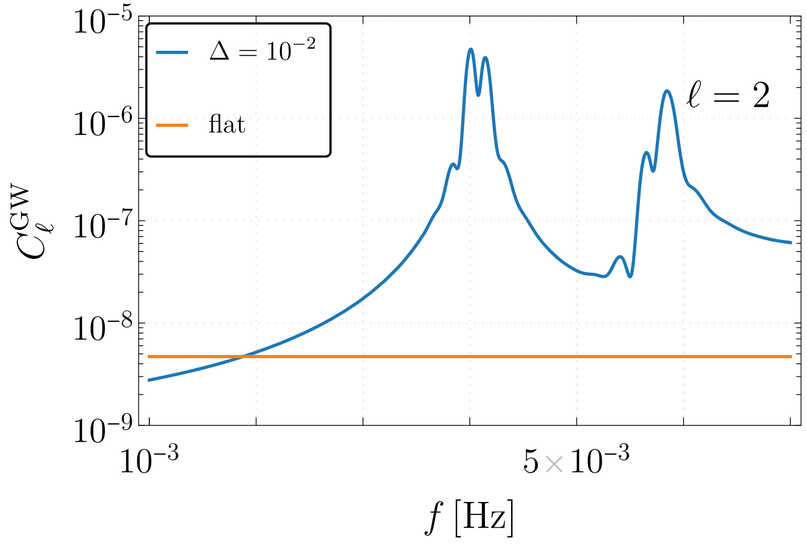

Kinematic (Doppler) anisotropies are a smoking-gun signal of extragalactic sources.

N. Bartolo et al., JCAP 11, 009 (2022); E. Dimastrogiovanni et al., JCAP 01, 018 (2023).

Kinematic anisotropies

The GW energy density in a boosted frame B moving with relative velocity $\vec{v}$ with respect to frame A is given by

$$\Omega_{\rm GW}^{(B)}(f,\hat{n}) = \frac{4\pi^2}{3\,H_0^2}\, f^3\, \mathscr{I}(f)\, \mathbf{P}_{\rm kin}(f,\hat{n}),$$

where

$$\mathbf{P}_{\rm kin}(f,\hat{n}) = \frac{\mathscr{D}}{\mathscr{I}(f)}\, \mathscr{I}(\mathscr{D}^{-1} f), \qquad \mathscr{D} = \frac{\sqrt{1-\beta^2}}{1-\beta\,\hat{n}\cdot\hat{v}}\,.$$

No anisotropies: $\mathbf{P}_{\rm kin}(f,\hat{n}) = 1.$

ET response function:

$$\mathscr{R}_{\mathscr{O},\mathscr{O}'}(f,t,t') = \frac{4}{5}\left[1+\frac{5}{2}c_1(f)\right]\, d^{ab}_{\mathscr{O}}(t)\, d_{\mathscr{O}'\,ab}(t') + \, c_2(f)\, \left(\hat{v}_a\, d^{ab}_{\mathscr{O}}(t)\, d_{\mathscr{O}'\,bc}(t')\, \hat{v}^c\right) + c_3(f)\, \left(\hat{v}^a\hat{v}^b\, d_{ab\,\mathscr{O}}(t)\right)\, \left(\hat{v}^c\hat{v}^d\, d_{cd\,\mathscr{O}'}(t')\right).$$

G. Cusin and G. Tasinato, JCAP 08, 036 (2022); ***D. Chowdhury et al., Phys. Rev. D 107, 083516 (2023).***

Kinematic anisotropy coefficients

Power-law

A single power-law SGWB profile:

$$\mathcal{I}^{PL}(f) = I_0 \left(\frac{f}{f_\star}\right)^\alpha ,$$

$$\Longrightarrow \mathbf{P}_{\rm kin} = \mathscr{D}^{1-\alpha} .$$

Example: $\alpha = 3$

$$c_1 = \frac{64}{105}\frac{\beta^2}{1-\beta^2} ,$$

$$c_2 = -\frac{4}{35}\frac{\beta^2}{1-\beta^2} ,$$

$$c_3 = 0 .$$

When $\beta = 0$, we get $c_i = 0 \forall i$ and $\forall \alpha$, as expected.

Curiously, we also find that $c_i = 0 \forall i$ when $\alpha = 1$, irrespective of the value of β.

D. Chowdhury et al., Phys. Rev. D 107, 083516 (2023).

Kinematic anisotropy coefficients

Power-law

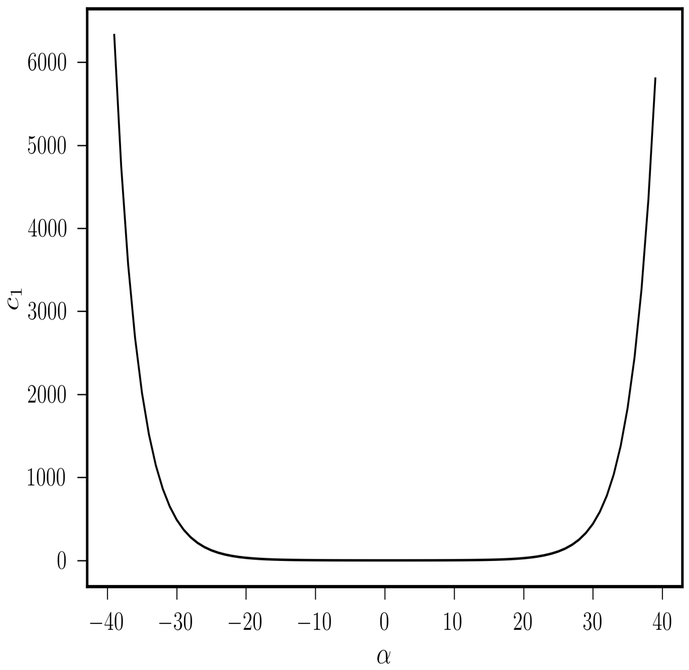

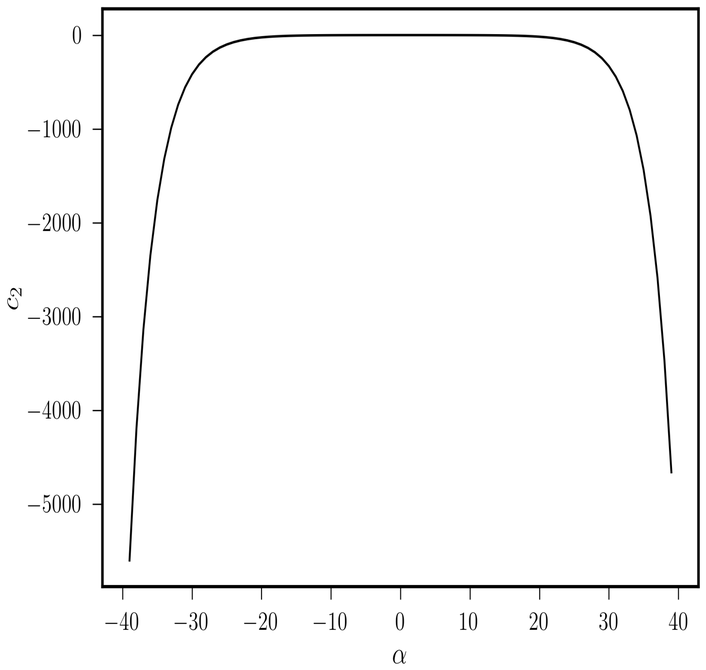

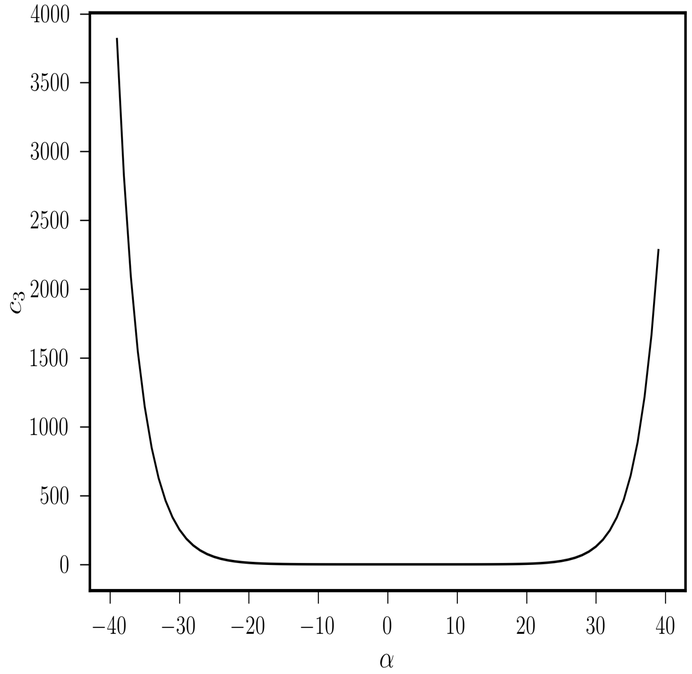

The coefficients c_i have been plotted for $\beta = 0.3$.

D. Chowdhury et al., Phys. Rev. D 107, 083516 (2023).

Kinematic anisotropy coefficients

Broken power-law

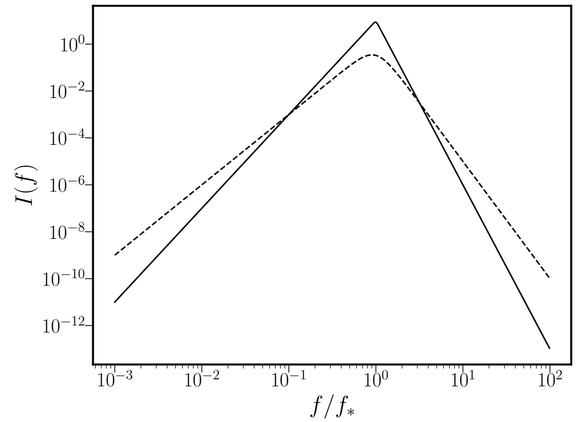

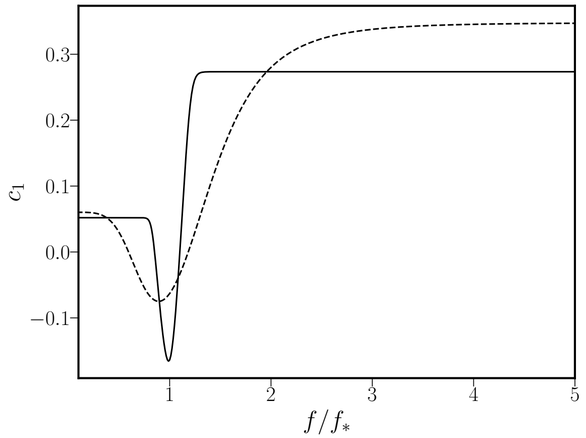

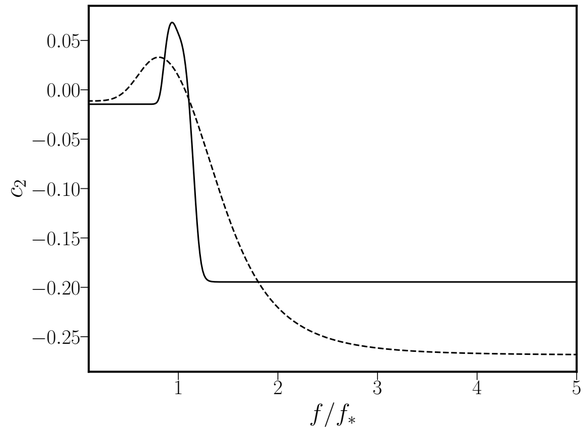

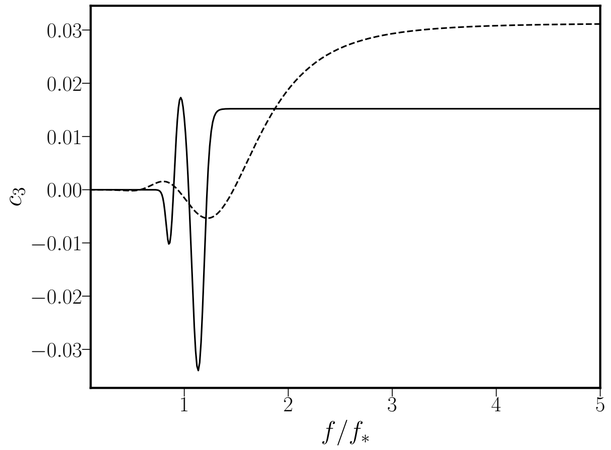

D. Chowdhury et al., Phys. Rev. D 107, 083516 (2023).

Kinematic anisotropy coefficients

Double power-law

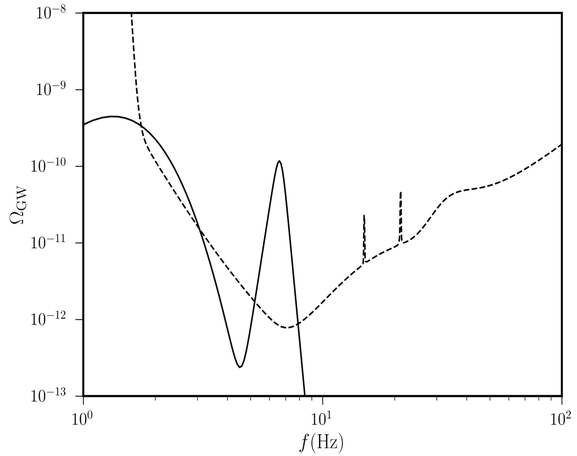

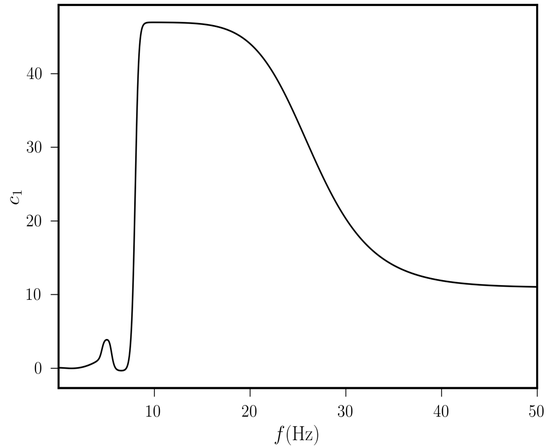

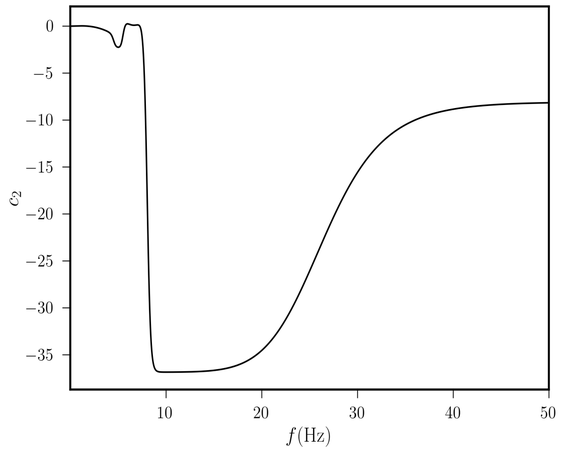

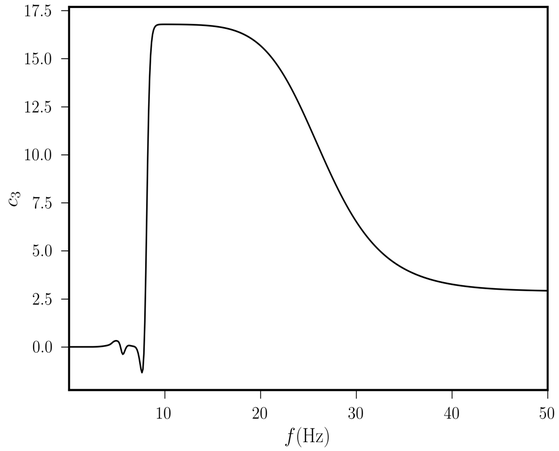

D. Chowdhury et al., Phys. Rev. D 107, 083516 (2023).

Detection prospects

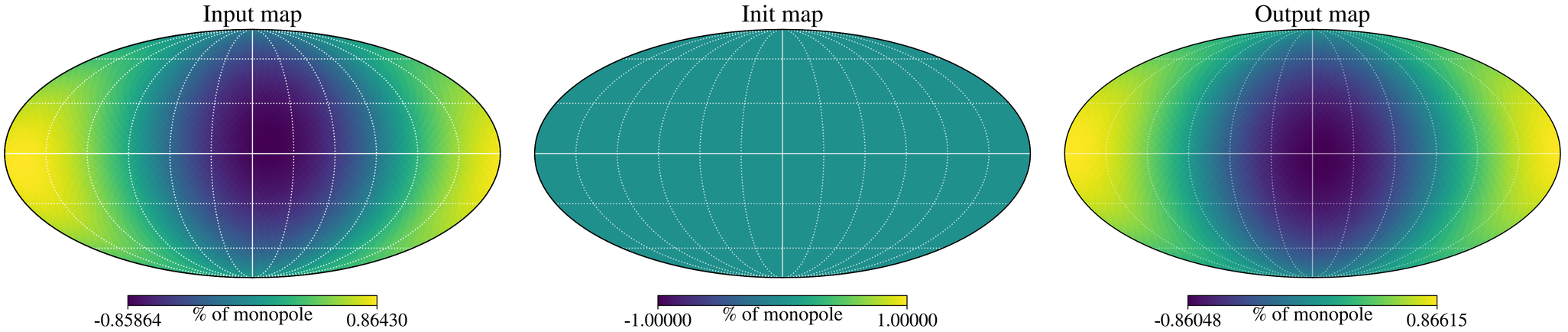

Plot from: L. Heisenberg et al., JCAP 01, 044 (2025).

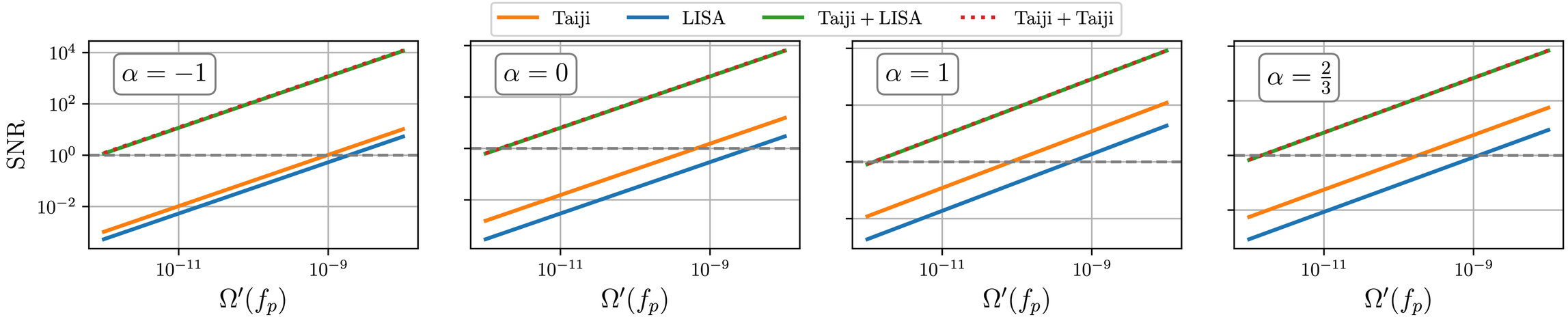

Plot from: Z.-C. Zhao and S. Wang, Sci. China Phys. Mech. Astron. 67, 120411 (2024).

Summary

- Primordial GWs are produced in various early-universe scenarios.
- Detecting the SGWB is one of the important aims of future detectors.
- It is important to be able to characterize the properties of the SGWB accurately.
- Anisotropies of the SGWB can provide further insights into early-universe phenomena.

Summary

- Primordial GWs are produced in various early-universe scenarios.
- Detecting the SGWB is one of the important aims of future detectors.
- It is important to be able to characterize the properties of the SGWB accurately.
- Anisotropies of the SGWB can provide further insights into early-universe phenomena.

Thank you!

LISA sources

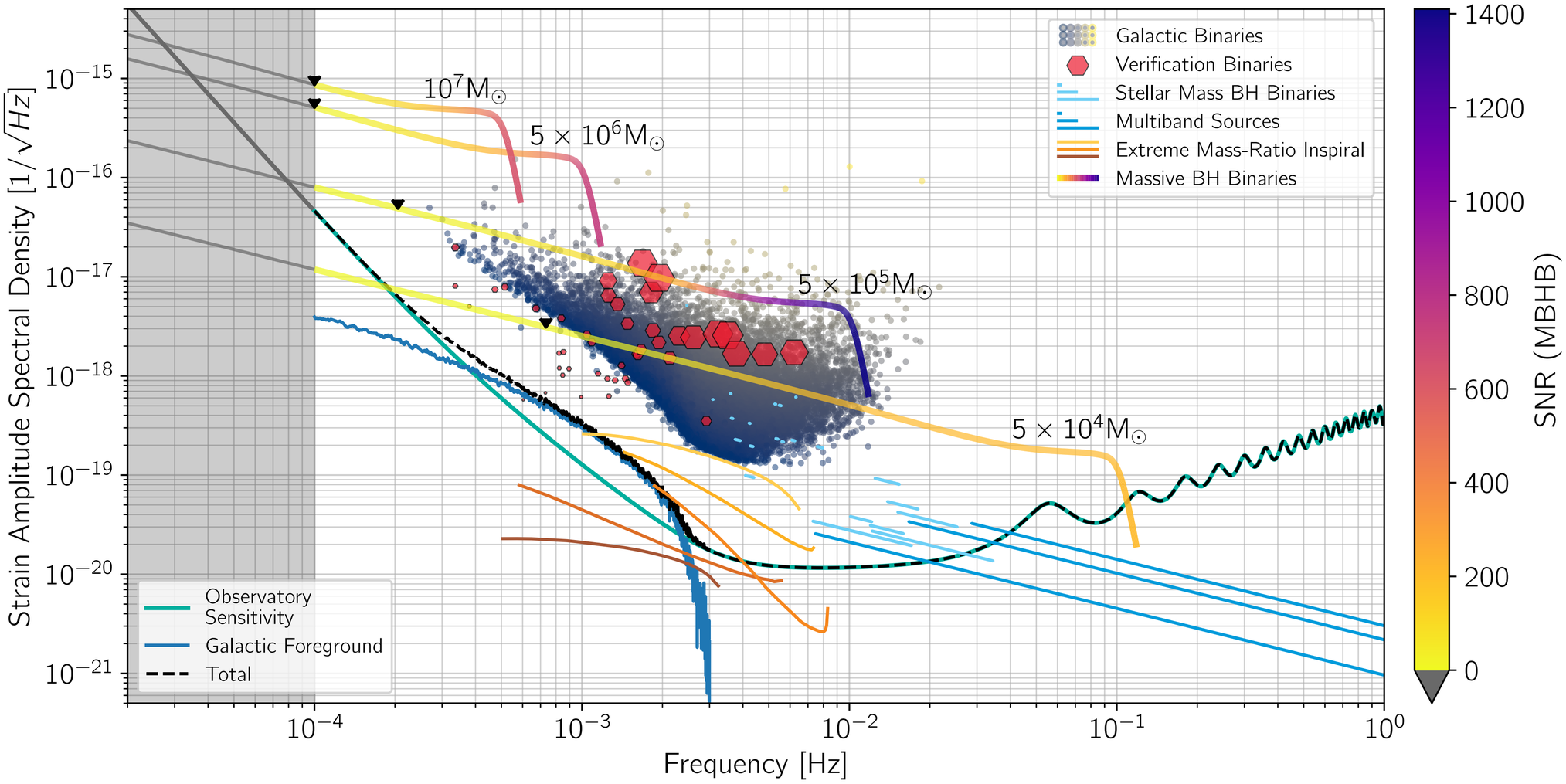

Plot from: LISA Collaboration, arXiv: 2402.07571 [astro-ph.CO] (2024).